Molecular Recognition of DNA by *Hoechst* Benzimidazoles: Exploring Beyond the Pyrrole-Imidazole-Hydroxypyrrole Polyamide-Pairing Code

by **Thomas G. Minehan**, **Konstanze Gottwald**, and **Peter B. Dervan***

Division of Chemistry and Chemical Engineering, California Institute of Technology, Pasadena, California 91125, USA

Dedicated to Professor *Albert Eschenmoser* on the occasion of his 75th birthday

A series of three-ring analogs of the minor-groove-binding molecule *Hoechst 33258* (**1**), consisting of benzimidazole (B), imidazopyridine (P), and hydroxybenzimidazole (H) monomers, have been synthesized in order to investigate both their sequence specificity and binding modes. MPE · Fe^{II} Footprinting has revealed the preference of both PBB and BBB ligands for 5′-WGWWW-3′ and 5′-WCWWW-3′ tracts, as well as A · T-rich sequences. Affinity-cleavage titrations show no evidence for a 2 : 1 binding mode of these *Hoechst* analogs. Importantly, all derivatives are oriented in one direction at each of their binding sites. The implications of these results for the design of minor-groove-binding small molecules is discussed.

1. Introduction. – Small molecules that bind DNA sequence specifically are important tools in molecular biology and may form the basis for novel classes of gene-targeted drugs directed toward cancer and infectious diseases [1][2]. The natural products netropsin (**N**) and distamycin A (**D**) are two- and three-ring *N*-methylpyrrolecarboxamides that bind in the minor groove of double-helical DNA at sites rich in A · T base pairs [3] (*Fig. 1*). X-Ray diffraction and NMR studies reveal that specificity is accomplished by these molecules as their 1 : 1 and 2 : 1 complexes with DNA depending on A · T sequence composition [4–10]. The synthetic dye *Hoechst 33258* (**1**) also binds double-helical DNA in the minor groove at sites rich in A · T base pairs [11]. The size and crescent shape of the *Hoechst* molecule **1** is similar to that of netropsin (**N**) and distamycin (**D**), and, indeed, these molecules all share common binding sites consisting of four to five consecutive A · T base-pairs as revealed by MPE · Fe^{II} footprinting [12]. In addition, X-ray and NMR studies of **1** bound to DNA as a 1 : 1 complex [13–15] indicate how the molecule accomplishes recognition of DNA: similar to netropsin (**N**) and distamycin (**D**), specific H-bonds are formed between the benzimidazole NHs and adjacent adenine N(3)- and thymine O(2)-atoms on the floor of the minor groove. The binding preference for A · T base pairs is a result of the close contact of the aromatic H-atoms of the *Hoechst* molecule **1** and the floor of the minor groove, thus precluding the binding of the drug at G · C base pairs due to the presence of the exocyclic *N*(2)-amino group of guanine. In addition, the binding of **1** is stabilized by electrostatic interactions and extensive *van der Waals* contacts with the walls of the minor groove. Unlike distamycin (**D**), only 1 : 1 complexes of **1** and DNA have been described.

Efforts to alter the sequence specificity of the natural product distamycin (**D**) to allow recognition of G · C base pairs came to fruition with the discovery that the simple

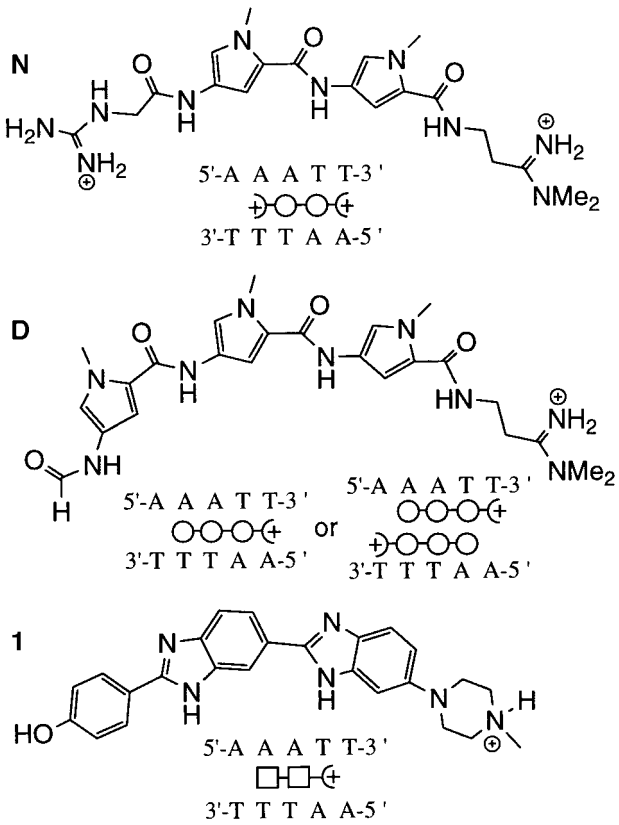

Fig. 1. *Structures and binding modes of the minor-groove-binding molecules netropsin* (**N**), *distamycin* (**D**), *and* Hoechst 33258 (**1**)

three-ring analog imidazole-pyrrole-pyrrole (ImPyPy; **2**) binds to a 5′-TGTCA-3′ site as an antiparallel side-by-side dimer in the minor groove [16][17]. The 2:1 model allowed specific contacts of the ligands with each strand on the floor of the minor groove, and it is the model from which the pairing rules for polyamide recognition of DNA arose (*Fig. 2*). Polyamides consisting of aromatic rings which differ only at the 3 position – imidazole (Im), pyrrole (Py), and hydroxypyrrole (Hp) – are now versatile ligands that can distinguish all four base pairs by a binary recognition code based on combinations of four building blocks: a Py/Im pair targets C·G, an Im/Py pair targets G·C, a Py/Hp pair targets A·T, and an Hp/Py pair targets T·A base pairs [18]. Analogs of *Hoechst 33258* (**1**) have been described in the literature [19], some of which are capable of recognizing G·C-containing sequences. However, although there has been evidence of cooperativity in the binding of **1** to DNA [20][21], there has been little investigation of the binding orientation of the derivatives of **1**. The goals of the present study were to rationally develop analogs of **1** that might allow recognition of DNA sequences of mixed A·T and G·C composition.

Our design of tris-benzimidazole derivatives of **1** was influenced by the current paradigm for polyamide recognition of DNA and, in particular, *Lown*'s contributions to

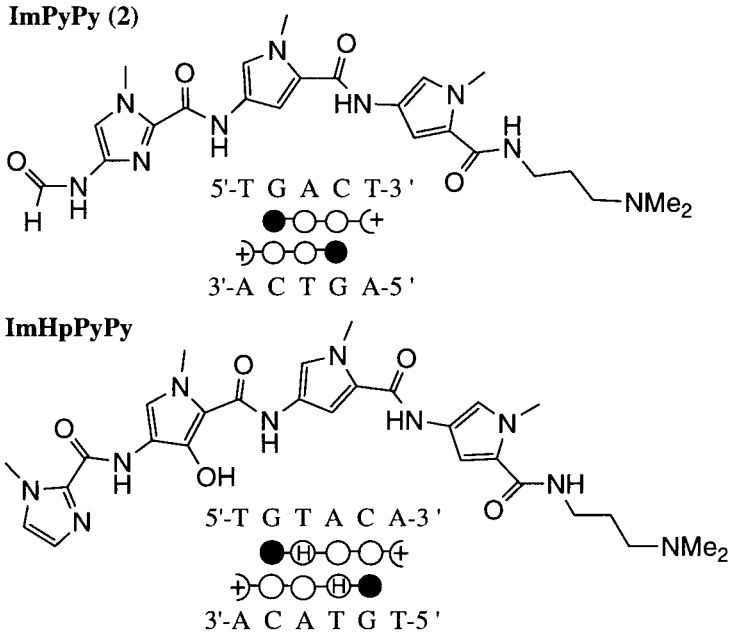

Fig. 2. *Structures and 2:1 binding modes of synthetic molecules which recognize DNA in the minor groove.* ImPyPy and ImHpPyPy bind 5′-TGACT-3′ and 5′-TGTACA-3′, respectively, as antiparallel homodimers. The pairing rules for polyamide recognition of DNA arose from study of the sequence specificity of these and similar molecules.

altered bis(benzimidazole) minor-groove binders [22] (*Fig. 3*). The benzimidazole (B), imidazopyridine (P), and hydroxybenzimidazole (H) monomers, which differ only at the 7-position, were envisioned to present an array of functionalities and H-bonding surfaces to the floor of the minor groove similar to pyrrole, imidazole, and hydroxypyrrole. It was anticipated that the imidazopyridine unit, containing a N-atom instead of the 7-CH of the benzimidazole nucleus, would bind opposite the G of a G·C base pair, and that the hydroxybenzimidazole unit, containing a C(7)–OH instead of the 7-CH, would bind opposite the T of a T·A base pair. An unmodified benzimidazole moiety would be degenerate for A·T and T·A base pairs. The trimers **3-Dp** (Dp: 3-(dimethylamino)propanamine; R = 4-MeOC$_6$H; R′ = Me) and **4-Dp** (R = 4-HOC$_6$H$_4$; R′ = Me), as *Hoechst 33258* (**1**) analogs of distamycin (**D**) and ImPyPy (**2**), were thus designed to investigate the sequence selectivity of these ligands relative to the parent molecules (*Fig. 4*). Resolution of the binding-site location and size can be accomplished by the method of MPE·Fe^{II} footprinting [23]. The affinity-cleaving analogs of **3-ED** and **4-ED** allow the binding mode and orientation of the ligands at their binding sites to be determined by affinity-cleavage titrations. An HBB trimer **5** was also designed to investigate the possibility of A·T/T·A discrimination by the derivatives of **1**.

In addition, although there have been numerous studies characterizing the exact binding sites of the parent compound **1** [11–15], there have been no reports on the orientation preferences of **1** at its binding sites. This information can be gained from

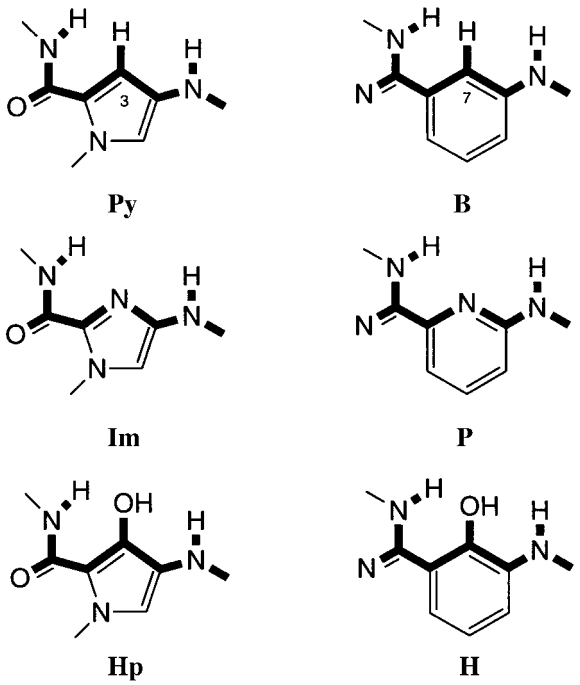

Fig. 3. *Rationale for the design of benzimidazole-based molecules for DNA recognition.* Similar H-bonding surfaces are presented to the floor of the minor groove for both the pyrrole-imidazole-hydroxypyrrole monomers and the benzimidazole-imidazopyridine-hydroxybenzimidazole monomers.

affinity cleavage of DNA with a simple derivative of **1** modified at its N-terminus with *Hoechst EDTA* (**1-ED**). We report here the synthesis of **1-ED** and characterization of its binding mode by affinity cleavage of pBr322 DNA.

2. Synthesis of Hoechst-EDTA (1-ED). – Tethering of the EDTA (ethylendiamine-*N*,*N*,*N*′,*N*′-tetraacetic acid) moiety from the *Hoechst* core was most easily accomplished by modifying the terminal piperazine unit (*Scheme 1*). Thus, 5-chloro-2-nitroaniline (**6**) was treated with piperazine in DMF in the presence of K_2CO_3 at elevated temperature to afford the corresponding piperazine-substituted nitroaniline. Reaction of this compound with ethyl bromoacetate and $EtN(i\text{-}Pr)_2$ in DMF overnight, followed directly by hydrogenation over Pd-C gave ethyl 4-(3,4-diaminophenyl)piperazine-1-acetate (**7**). Compound **7** was then coupled with carbaldehyde **9** under *Lown* conditions (*vide infra*) to afford ethyl ester **8**. Transformation to the EDTA derivative **1-ED** took place in three steps: hydrolysis of the ethyl ester and methyl ether of **8** with refluxing 48% HBr, amide-bond formation by *N*,*N*′-dicyclohexylcarbodiimide (DCC)/1-hydroxybenzotriazole (HOBt)-mediated coupling of the acid and *N*-methylpropane-1,3-diamine, and reaction of the terminal amine with EDTA-dianhydride as described below for the preparation of **3-ED** and **4-ED**. This sequence afforded **1-ED** in 5% overall yield, and the compound was characterized by UV and ^{1}H-NMR spectroscopy, and high-resolution mass spectrometry.

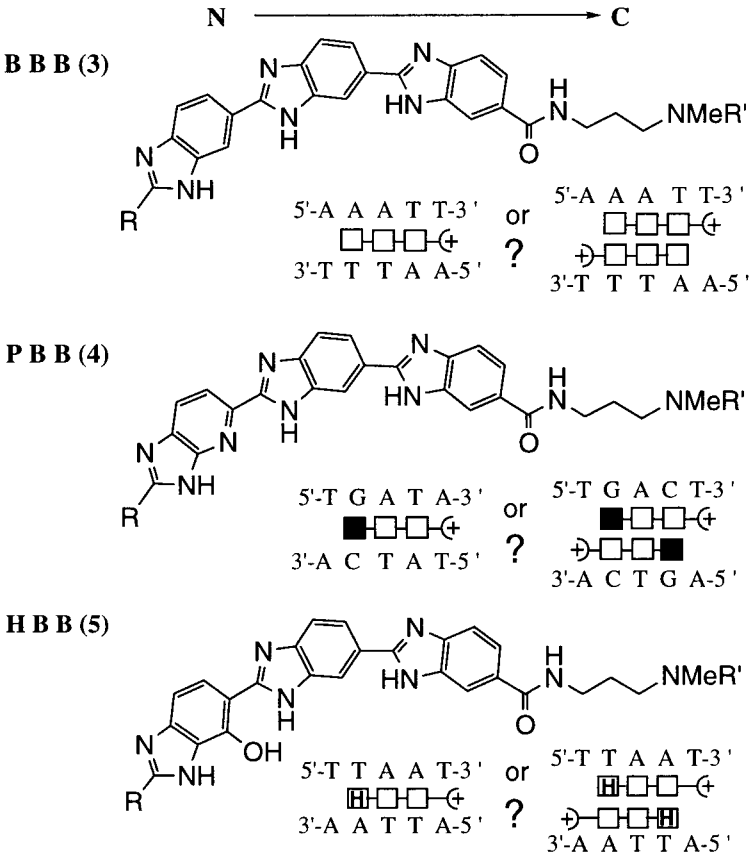

Fig. 4. *The BBB and PBB trimers,* **3** *and* **4**, *along with their affinity-cleaving analogs designed to investigate the binding mode and sequence selectivity of* Hoechst *derivatives.* The HBB trimer **5** was synthesized to investigate the possibility of A·T discrimination by *Hoechst* compounds.

3. Synthesis of the BBB and PBB Trimers, 3 and 4, Respectively. – Because of difficulties encountered at the monomer stage in the preparation of the imidazopyridine trimer with R = H (*Fig. 4*), it was decided, for synthetic ease, to construct the PBB and BBB trimers containing a 4-methoxyphenyl cap (R = 4-MeOC$_6$H$_4$; *Fig. 4*). As described by *Lee et al.*, 2-(4-methoxyphenyl)-1*H*-benzimidazole-6-carbaldehyde (**9**) was prepared from methyl 3,4-dinitrobenzoate [24]; 2-(4-methoxyphenyl)-1*H*-imidazo[5,4-*b*]pyridine-6-carbaldehyde (**10**) was prepared from 2-amino-6-methylpyridine according to the procedure of *Lown* and co-workers [25] (*Scheme 2*). Coupling of **10** with diamino compound **11** [26] was accomplished by refluxing the mixture in PhNO$_2$ at 150° for 19–24 h under Ar. Evaporation of the solvent, trituration with Et$_2$O/CH$_2$Cl$_2$, and filtration conveniently afforded the trimer **13** as a brown solid in 51% yield. This method was also used to construct trimer **12** in 62% yield from **11** and **9**. A variety of different methods were attempted in order to hydrolyze the CN group of **12** and **13**. Basic conditions at elevated temperatures resulted in extensive decomposition of the

Scheme 1. *Synthesis of* Hoechst-EDTA (**1-ED**)

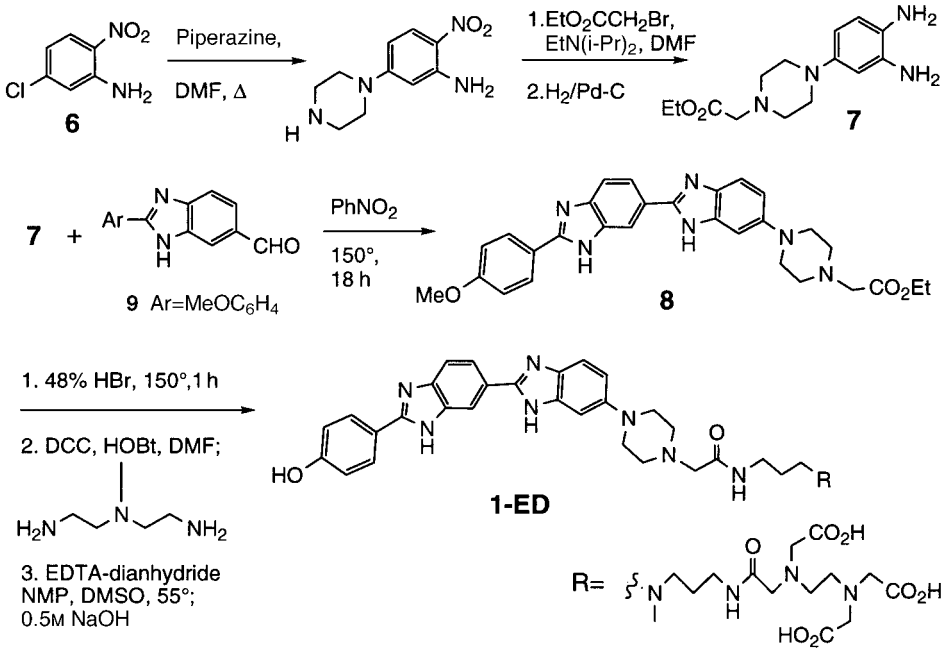

Scheme 2. *Synthesis of PBB and BBB Trimers and Their Affinity-Cleaving Analogs*

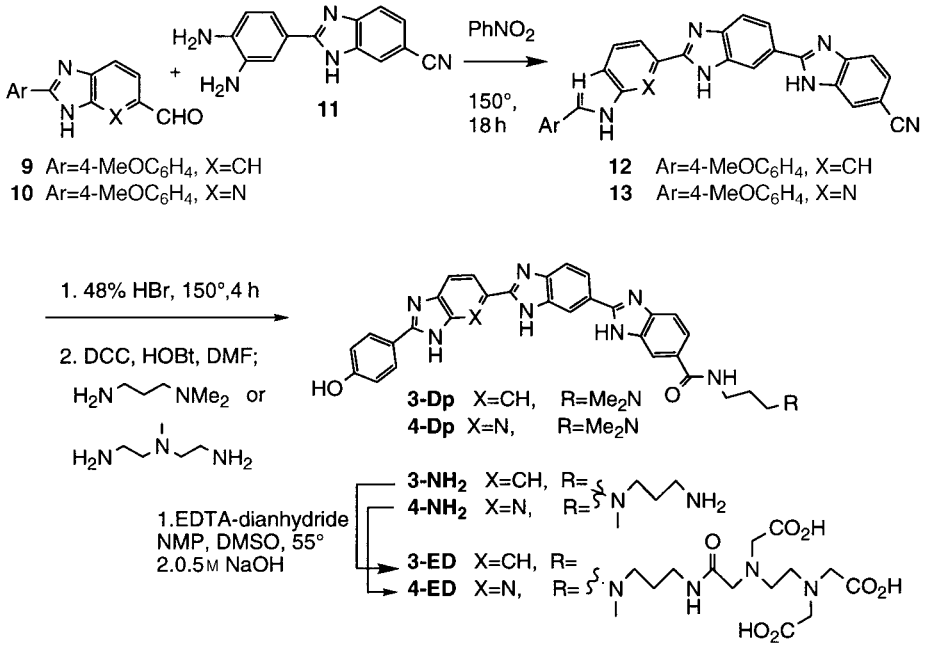

trimers. Treatment of the carbonitriles with 75% H_2SO_4 for 1 h at 150° resulted in hydrolysis of the carbonitrile to carboxylic acid accompanied by partial hydrolysis of the aromatic methyl ether. Extended treatment with 75% H_2SO_4 resulted in decomposition. However, it was found that hydrolysis with 48% HBr at 130° for 4 h resulted in clean conversion to the intermediate hydroxyphenyl carboxylic acids. The crude acids were immediately coupled under DCC/HOBt conditions at room temperature with either *N,N*-dimethylpropane-1,3-diamine or $MeNPr_2$ to afford amides **3-Dp**,**4-Dp**, and **3-NH$_2$**,**4-NH$_2$**, respectively. The EDTA derivatives for PBB and BBB were prepared from **3-NH$_2$** and **4-NH$_2$** by treatment with EDTA dianhydride in DMSO/*N*-methylphthalimide (NMP) solution at 55° for 5 min, followed by hydrolysis with 0.1N NaOH and 55° for 10 min and subsequent HPLC purification [27]. The identity of all compounds was confirmed by UV and ^{1}H-NMR spectroscopy, and high-resolution mass spectrometry.

4. Synthesis of the HBB Trimer 5. – In the initial approach to the HBB trimer, it was found that the most convenient starting material, which contains the aromatic substitution pattern required for synthesis of the hydroxybenzimidazole subunit, was the methyl carboxylate **14** (*Scheme 3*). Furthermore, for synthetic ease, a 2-Me-substituted terminal benzimidazole unit was selected as the capping moiety of our target molecule. A convenient route to carbaldehyde **15** was developed, in which a one-pot nitro reduction/acid-catalyzed cyclization/dehydration of **14** produced the intermediate 2-methylbenzimidazole-carboxylate, which was subsequently reduced and oxidized according to the procedure described in [28]. Coupling of **15** and **11** in refluxing

Scheme 3. *Synthesis of the HBB Trimer* **5**

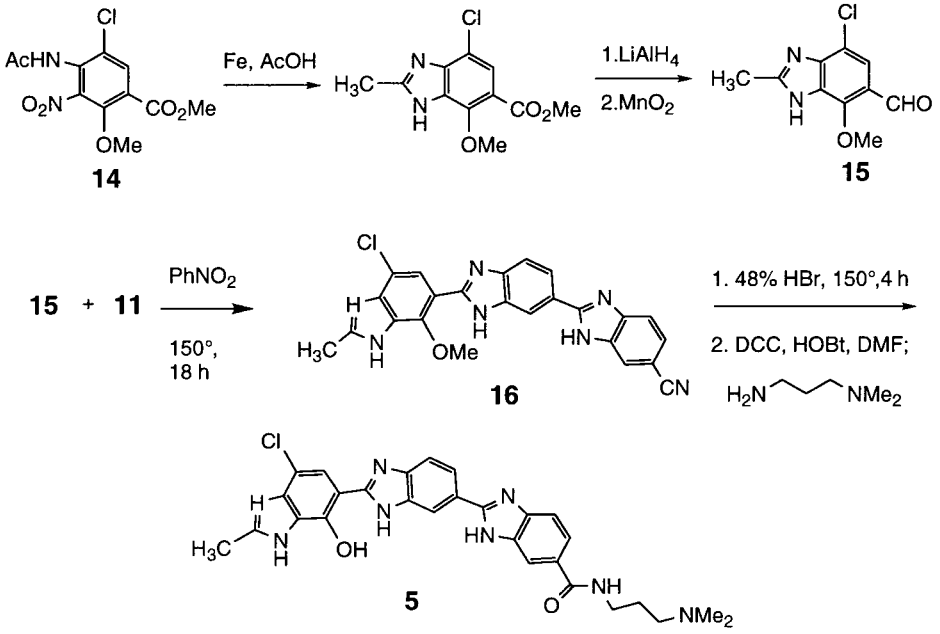

$PhNO_2$ at 150° took place smoothly to afford the benzimidazole-carbonitrile **16** in 78% yield. Nitrile and methyl-ether hydrolysis followed by direct coupling of the crude acid under DCC/HOBt conditions with *N*,*N*-dimethylpropane-1,3-diamine afforded trimer amide **5** in 20% yield after HPLC purification. The identity of all compounds was confirmed by UV and ^{13}C-NMR spectroscopy, and high-resolution mass spectrometry.

5. Analysis of Binding-Site Location and Size by MPE · Fe(II) Footprinting. – The 519 base-pair EcoRI/RsaI restriction fragment of plasmid pBr322 has been used extensively for characterization of the sequence selectivity of the parent molecules distamycin (**D**), ImPyPy-Dp (**2-Dp**) [16], and *Hoechst 33258* (**1**) [12], and thus was also selected the present study. MPE · Fe(II) footprinting of **1**, **2-Dp**, **3-Dp**, and **4-Dp** on 3′-^{32}P-end-labeled 519-bp restriction fragment reveals similarities in the binding-site locations of all the benzimidazole-based ligands (*Fig. 5*, *a* and *c*). Both PBB (lanes *11*–*13*) and BBB (lanes *14*–*16*) bind the 5–6 base-pair sequences 5′-TAAGA-3′, 5′-TTATTA-3′, 5′-TTAACC-3′, and 5′-TATCA-3′, sites which they also have in common with **1**. In contrast, a single footprint for **2-Dp** at the site 5′-TGACA-3′ is observed, and neither **3-Dp** nor **4-Dp** bind at this location. Although quantitative evaluation of the binding affinities for these ligands for their match sites by DNase footprinting was not performed, comparison of the intensity of the protection patterns for 20 μM **2-Dp** at the site 5′-TGACA-3′ with that for 10 μM **4-Dp** and 10 μM **3-Dp** at the site 5′-AGAAA-3′ suggests that, regardless of binding mode, **4-Dp** and **3-Dp** have higher affinities for their respective binding sites than **2-Dp**. Footprints for these compounds were also compared on the 5′-^{32}P PCR-labeled 3991–4143 segment of pBr322 (*Fig. 6*, *a* and *c*). Again, both PBB and BBB bind the same sites, which can be summarized as 5′-WWWWCC-3′, 5′-WWWWC(W)-3′, 5′-WWWWG-3′, 5′-WWWCW-3′, and 5′-WWWGW-3′. Remarkably, the sites 5′-WWWGW-3′ and 5′-WWWCW-3′ (from the previous experiment) are bound equally well by **3-Dp** and **4-Dp**. Several conclusions can be drawn from these data. First, although the PBB trimer differs from the BBB trimer in the terminal monomer unit by the substitution of the N-atom for an aromatic CH, the two ligands do not seem to have different DNA-sequence preferences. This may be due to free rotation about the C–C bond connecting the terminal and penultimate benzimidazole residues, allowing surfaces from both the convex and concave faces of the ligand to be presented to the floor of the minor groove. Second, since neither PBB nor BBB bind 5′-TGACA-3′, and since they occupy virtually identical binding sites to **1**, this suggests a likely 1:1 binding mode for these tris[benzimidazole] ligands. Affinity-cleavage experiments verified this hypothesis.

MPE Footprinting of the HBB trimer was performed on a 286-bp fragment of the plasmid pJT3 [29] (data not shown), which contains cassettes of five consecutive As or Ts. If HBB can discriminate a T base pair from an A base pair, fewer footprints should be seen than for the parent *Hoechst* compound **1**. HBB showed very weak footprints, even at 100 μM; comparison with **1** showed that both molecules bind to identical sequences. Since the HBB trimer has a low affinity for DNA and apparently does not discriminate T from A, no further experiments were performed with this compound; other trimer derivatives containing simple substituted hydroxyphenyl rings in the terminal position are currently being investigated, and footprinting results will be reported in due course.

6. Analysis of Binding Mode and Orientation by Affinity-Cleavage Titration. – The affinity-cleavage gel and histograms for ImPyPy-ED (**2-ED**) (*Lanes 6* and *7*, *Fig. 5*, *b* and *d*) show a symmetrical pattern of cleavage on both sides of the single site 5′-TGACA-3′, indicative of a 2 : 1 binding mode for **2-ED** at this site. In contrast, *Hoechst*-ED (**1-ED**, *Lanes 4* and *5*), BBB-ED (**3-ED**, *Lanes 8* and *9*), and PBB-ED (**4-ED**, *Lanes 10* and *11*) show strong cleavage patterns on only one side of each binding site. Thus, both tris[benzimidazole] compounds, as well as the parent molecule **1**, appear to bind DNA with 1 : 1 stoichiometry; *surprisingly, however, these data also indicate that all three ligands are oriented in one particular direction when bound*. Because of the proximity of some binding sites, especially for *Hoechst*-ED (**1-ED**), cleavage patterns at adjacent sites often overlap so that assignment of ligand orientation in some cases is inferred from the absence of a strong cleavage pattern on the other side of the binding site (*Fig. 7*, *a*). Interestingly, comparison of the loci of cleavage for **3-ED** and **4-ED** at their common binding sites indicates *that at some sites, the orientation of PBB and BBB are opposite* (see the upper portion of the gel in *Fig. 5*, *b*). This is even more evident in the affinity cleavage of the 5′-^{32}P PCR-labeled 3991 – 4143 segment of pBr322 with **3-ED** and **4-ED** (*Fig. 6*, *b* and *d*): PBB-ED shows a cleavage pattern to the 3′ side of 5′-ATTTCC-3′, whereas BBB-ED shows a cleavage pattern to the 5′ side of the same site. There are several other examples of sequences where this is also the case; a summary of the binding sites and orientations of **1-ED**, **3-ED**, and **4-ED** is shown in *Fig. 7*. Although there are no obvious alignment trends for each ligand, it seems that in many instances, the terminal benzimidazole/pyridimidazole-phenol portion of the molecule prefers to lie next to a G · C base-pair. Perhaps the freely rotating phenol moiety prefers the wider minor groove associated with G · C base-pairs. These data indicate that steric and/or *van der Waals* interactions may be more important than H-bond formation in the molecular recognition of DNA by *Hoechst 33258* (**1**) and its derivatives.

7. Discussion and Conclusion: The Different DNA-Binding Properties of Polyamides and Bis- and Tris[benzimidazoles]. – CPK Models of distamycin (**D**) and BBB (**3**) show a difference in the curvature of the two crescent-shaped molecules. As with models of ImPyPy (**2**) and PBB (**4**), there is consistently a greater degree of curvature for the polyamide than for the tris[benzimidazole] in the same series. Gas-phase minimizations of molecular models also corroborate this observation [30]. However, the curvature of PBB (**4**) and distamycin (**D**) are quite similar, thus making it difficult to draw any conclusions concerning modes of binding for an entire class of ligands from these observations. Experimentally, MPE · Fe^{II} footprinting data indicate the similar binding site preferences of *Hoechst* compound **1** and the PBB and BBB trimers, and also distinguish these three molecules from ImPyPy, both in affinity and sequence specificity. The higher affinity of benzimidazoles for the DNA sequences studied may indicate the existence of strong, favorable associations (*van der Waals* interactions) between the ligand and the walls of the minor groove at the binding site. Indeed, the benzimidazole-monomer unit has a greater aromatic surface area for such contacts than either pyrrole or imidazole. These interactions may further suggest an explanation for the affinity cleavage data, in which *Hoechst*-ED (**1-ED**), PBB-ED (**4-ED**), and BBB-ED (**3-ED**) are clearly distinguished from ImPyPy-ED (**2-ED**) in binding mode. The strong associations with the minor groove formed upon binding of the first molecule of

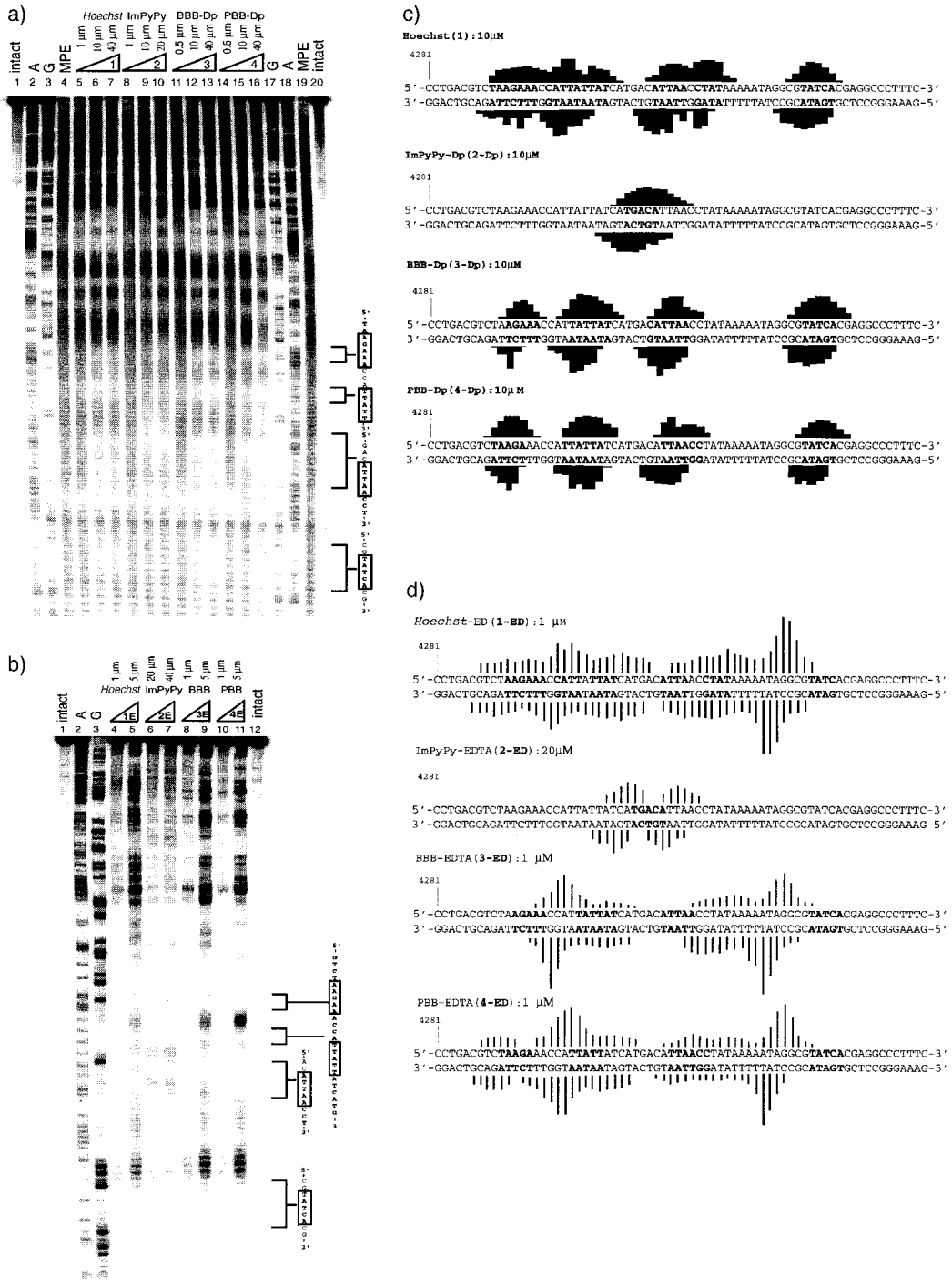
a)
Hoechst ImPyPy BBB-Dp PBB-Dp
intact A G MPE 1 µm 10 µm 40 µm 1 µm 10 µm 30 µm 0.5 µm 10 µm 40 µm 0.5 µm 10 µm 40 µm G A MPE intact
1 2 3 4 5 6 7 8 9 10 11 12 13 14 15 16 17 18 19 20
1 2 3 4
b)
1 µm 5 µm 20 µm 40 µm 1 µm 5 µm 1 µm 5 µm
Hoechst ImPyPy BBB PBB
intact A G 1E 2E 3E 4E intact
1 2 3 4 5 6 7 8 9 10 11 12
c)
Hoechst(1):10µM
ImPyPy-Dp(2-Dp):10µM
BBB-Dp(3-Dp):10µM
PBB-Dp(4-Dp):10µM
4281
5′-CCTGACGTCTAAGAAACCATTATTATCATGACATTAACCTATAAAAATAGGCGTATCACGAGGCCCTTTC-3′
3′-GGACTGCAGATTCTTTGGTAATAATAGTACTGTAATTGGATATTTTTATCCGCATAGTGCTCCGGGAAAG-5′
d)
Hoechst-ED(1-ED):1 µM
ImPyPy-EDTA(2-ED):20µM
BBB-EDTA(3-ED):1 µM
PBB-EDTA(4-ED):1 µM
4281
5′-CCTGACGTCTAAGAAACCATTATTATCATGACATTAACCTATAAAAATAGGCGTATCACGAGGCCCTTTC-3′
3′-GGACTGCAGATTCTTTGGTAATAATAGTACTGTAATTGGATATTTTTATCCGCATAGTGCTCCGGGAAAG-5′

bis- or tris[benzimidazole] may discourage the binding of a second molecule at the same site (in either a stacked antiparallel, parallel, or slipped mode). In addition, tris[benzimidazole] ligands may prefer A·T tracts, 5′-WGWWW-3′, and 5′-WCWWW-3′ sites, because the narrow minor-groove walls at these locations can hug the ligand, maximizing the favorable *van der Waals* interactions. The sequence-dependent variation in the width of the minor groove must also be considered in the discussion of ligand orientational preferences at individual binding sites. Virtually all of the sites bound by the *Hoechst* compound, PBB, and BBB have a G·C base pair at the end, which serves to slightly widen the otherwise narrow A·T tract. As discussed above, all three molecules adopt an orientation in which the N-terminus is positioned close to the G·C base pair, likely because of the greater steric space required by a freely rotating phenol moiety. It is difficult, however, to rationalize the observation that, at certain sequences, PBB and BBB, which differ only by the single atomic substitution of N for CH, adopt different orientations. Perhaps local dipole moments in the minor groove may exert differential orienting effects on the different ligands.

These studies demonstrate that much is still unknown about the factors responsible for sequence selectivity, orientation, binding mode and affinity of *Hoechst* derivatives which bind in the minor groove of DNA.

We are grateful for financial support from the *National Institutes of Health*, the *Beckman Institute*, *BASF*, and *Studienstiftung des deutschen Volkes* for a postdoctoral fellowship to *K. G.*, and the *American Cancer Society* for a postdoctoral fellowship to *T. G. M.*. We also wish to thank *Victor Rucker* for performing gas-phase minimizations on distamycin, ImPyPy, PBB, and BBB.

Experimental Part

1. General. – *Abbreviations:* DCC: 1,3-Dicyclohexylcarbodiimide, DIEA: $EtN(i\text{-}Pr)_2$, Dp: 3-(Dimethylamino)propylamine, HOBt: 1-Hydroxy-1*H*-benzotriazole, FC: flash chromatography. *Reagents and Equipment:* Solvents and reagents were purchased from *Aldrich* of the highest quality available and were used without further purification. TLC: *Merck* silica gel *60-F_{254}* anal. plates. FC: *Baker* silica gel (40 μm). Anal. reversed-phase (RP) HPLC: *Hewlett-Packard 1090 Liquid Chromatograph* or *Beckman System Gold* (detector *168*, solvent module *125*), flow 1 ml/min, UV detector at λ 280–340 nm, *Varian Microsorb-MV 100 Å C18* column 4.6 × 250 mm, linear gradient: 0.1% CF_3COOH/H_2O (*A*), MeCN (*B*), 0 min 0% *B*, 30 min 60% *B*, 35 min 100% *B*; t_R values refer to anal. HPLC. Prep. RP-HPLC: *Beckman System Gold* (detector *166P*, solvent module *127P*), flow 8 ml/min, UV detector at λ 280–340 nm, *Waters PrepLC* 25-mm module *C18* column, linear gradient: 0.1% CF_3COOH/H_2O (*A*), MeCN (*B*), 0 min 0% *B*, 5 min 0% *B*, 45 min 20% *B*, 85 min 30% *B*, 95 min 35% *B*, 97 min 50% *B*, 100 min 95% *B*. UV: *Hewlett-Packard 8452* diode-array spectrophotometer, λ_{max} in nm, ε in M^{-1} cm^{-1}.

◀

Fig. 5. a) *MPE-Fe^{II} Footprinting of* Hoechst 33258 (**1**), *ImPyPy-Dp* (**2-Dp**), *BBB-Dp* (**3-Dp**) *and PBB-Dp* (**4-Dp**) *trimers on the 3′-end-labelled 519-bp EcoRI/RsaI restriction fragment of PBr322: Lanes 1* and *20:* intact 3′-labeled DNA; *Lanes 2–3* and *17–18:* A and G reactions; *Lanes 4* and *19:* MPE-Fe^{II} digestion of DNA in the absence of ligand; *Lanes 5–7, 1, 20:* 40 μM *Hoechst*; *Lanes 8–10, 1, 10:* 20 μM ImPyPy-Dp; *Lanes 11–13:* 0.5, 10, 40 μM BBB-Dp; *Lanes 14–16:* 0.5, 10, 40 μM PBB-Dp. b) *Affinity cleavage of the 519-bp EcoRI/RsaI restriction fragment of pBr-322 with* Hoechst-EDTA (**1-ED**), *ImPyPy-ED* (**2-ED**), *BBB-ED* (**3-ED**), *and PBB-ED* (**4-ED**). *Lanes 1 and 12:* intact 3′-labeled DNA; *Lanes 2–3:* A and G reactions; *Lanes 4 and 5:* 1 and 5 μM *Hoechst-ED; Lanes 6* and *7:* 20 and 40 μM ImPyPy-ED; *Lanes 8* and *9:* 1 and 5 μM BBB-ED; *Lanes 10* and *11:* 1 and 5 μM PBB-ED. c) *Binding sites* (in bold) *as determined by MPE-Fe^{II} footprinting, shown on the 5′ and 3′-end labelled 4281–4350 segment of PBr322*. Bar heights are proportional to the relative protection from cleavage at each band. Shown are the protection patterns for 10 μM *Hoechst*, 20 μM ImPyPy-Dp, 10 μM BBB-Dp, and 10 μM PBB-Dp on the 4281–4350 segment of PBr322. d) *Affinity-cleavage patterns for 1* μM Hoechst-*ED, 20* μM *ImPyPy-ED, 1* μM *BBB-EDTA, and 1* μM *BBB-ED on the 4281–4350 segment of PBr322*. Line heights are proportional to the relative cleavage at each band; binding sites (as determined above) are in bold.

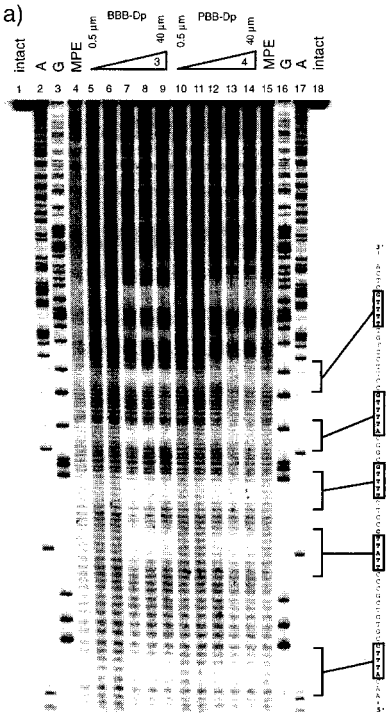
a)
BBB-Dp
PBB-Dp
intact
A
G
MPE
0.5 μm
40 μm
3
4
1 2 3 4 5 6 7 8 9 10 11 12 13 14 15 16 17 18

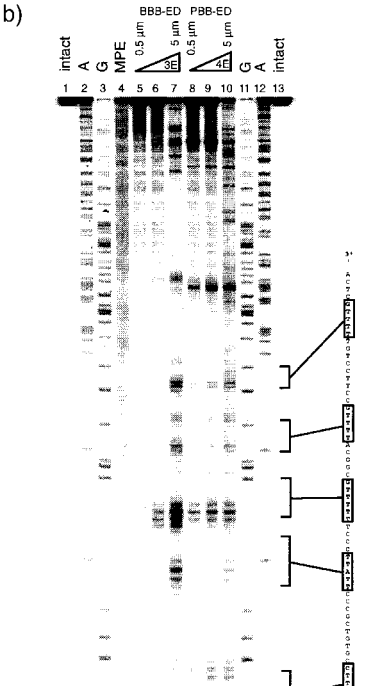
b)
BBB-ED
PBB-ED
intact
A
G
MPE
0.5 μm
5 μm
3E
4E
1 2 3 4 5 6 7 8 9 10 11 12 13

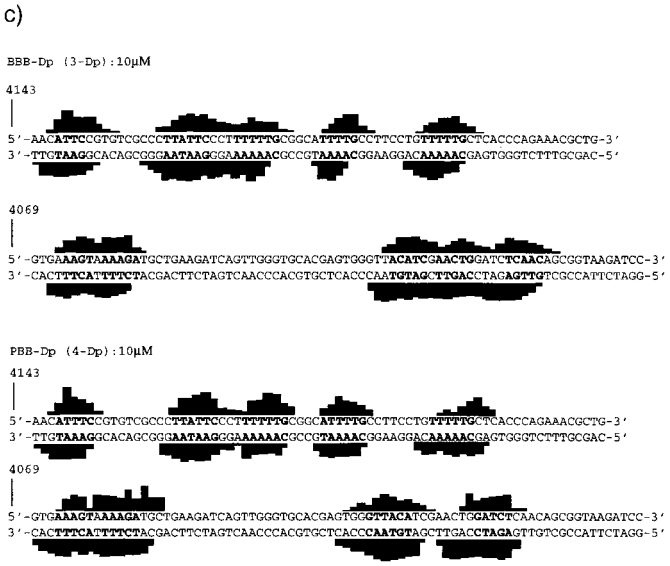
c)
BBB-Dp (3-Dp):10μM
4143
5′-AACATTCCGTGTCGCCCTTATTCCCTTTTTTGCGGCATTTTGCCTTCCTGTTTTTGCTCACCCAGAAACGCTG-3′
3′-TTGTAAGGCACAGCGGGAATAAGGGAAAAAACGCCGTAAAACGGAAGGACAAAAACGAGTGGGTCTTTGCGAC-5′
4069
5′-GTGAAAGTAAAAGATGCTGAAGATCAGTTGGGTGCACGAGTGGGTTACATCGAACTGGATCTCAACAGCGGTAAGATCC-3′
3′-CACTTTCATTTTCTACGACTTCTAGTCAACCCACGTGCTCACCCAATGTAGCTTGACCTAGAGTTGTCGCCATTCTAGG-5′
PBB-Dp (4-Dp):10μM
4143
5′-AACATTTCCGTGTCGCCCTTATTCCCTTTTTTGCGGCATTTTGCCTTCCTGTTTTTGCTCACCCAGAAACGCTG-3′
3′-TTGTAAAGGCACAGCGGGAATAAGGGAAAAAACGCCGTAAAACGGAAGGACAAAAACGAGTGGGTCTTTGCGAC-5′
4069
5′-GTGAAAGTAAAAGATGCTGAAGATCAGTTGGGTGCACGAGTGGGTTACATCGAACTGGATCTCAACAGCGGTAAGATCC-3′
3′-CACTTTCATTTTCTACGACTTCTAGTCAACCCACGTGCTCACCCAATGTAGCTTGACCTAGAGTTGTCGCCATTCTAGG-5′

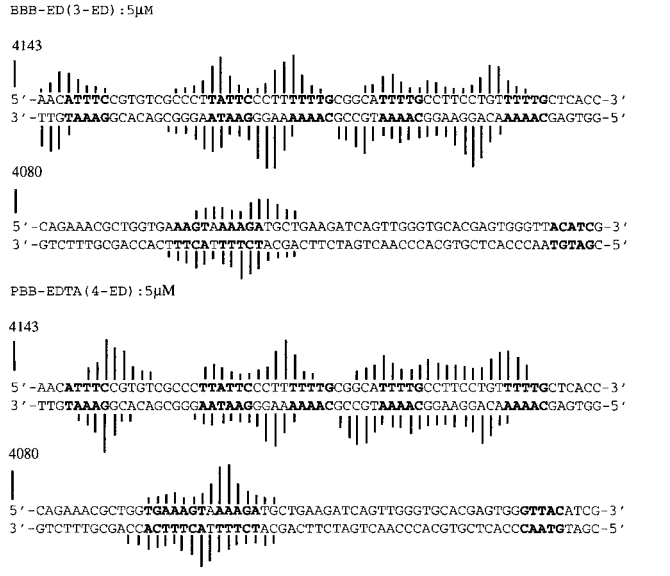
d)
BBB-ED(3-ED):5μM
4143
5′-AACATTTCCGTGTCGCCCTTATTCCCTTTTTTGCGGCATTTTGCCTTCCTGTTTTTGCTCACC-3′
3′-TTGTAAAGGCACAGCGGGAATAAGGGAAAAAACGCCGTAAAACGGAAGGACAAAAACGAGTGG-5′
4080
5′-CAGAAACGCTGGTGAAAGTAAAAGATGCTGAAGATCAGTTGGGTGCACGAGTGGGTTACATCG-3′
3′-GTCTTTGCGACCACTTTCATTTTCTACGACTTCTAGTCAACCCACGTGCTCACCCAATGTAGC-5′
PBB-EDTA(4-ED):5μM
4143
5′-AACATTTCCGTGTCGCCCTTATTCCCTTTTTTGCGGCATTTTGCCTTCCTGTTTTTGCTCACC-3′
3′-TTGTAAAGGCACAGCGGGAATAAGGGAAAAAACGCCGTAAAACGGAAGGACAAAAACGAGTGG-5′
4080
5′-CAGAAACGCTGGTGAAAGTAAAAGATGCTGAAGATCAGTTGGGTGCACGAGTGGGTTACATCG-3′
3′-GTCTTTGCGACCACTTTCATTTTCTACGACTTCTAGTCAACCCACGTGCTCACCCAATGTAGC-5′

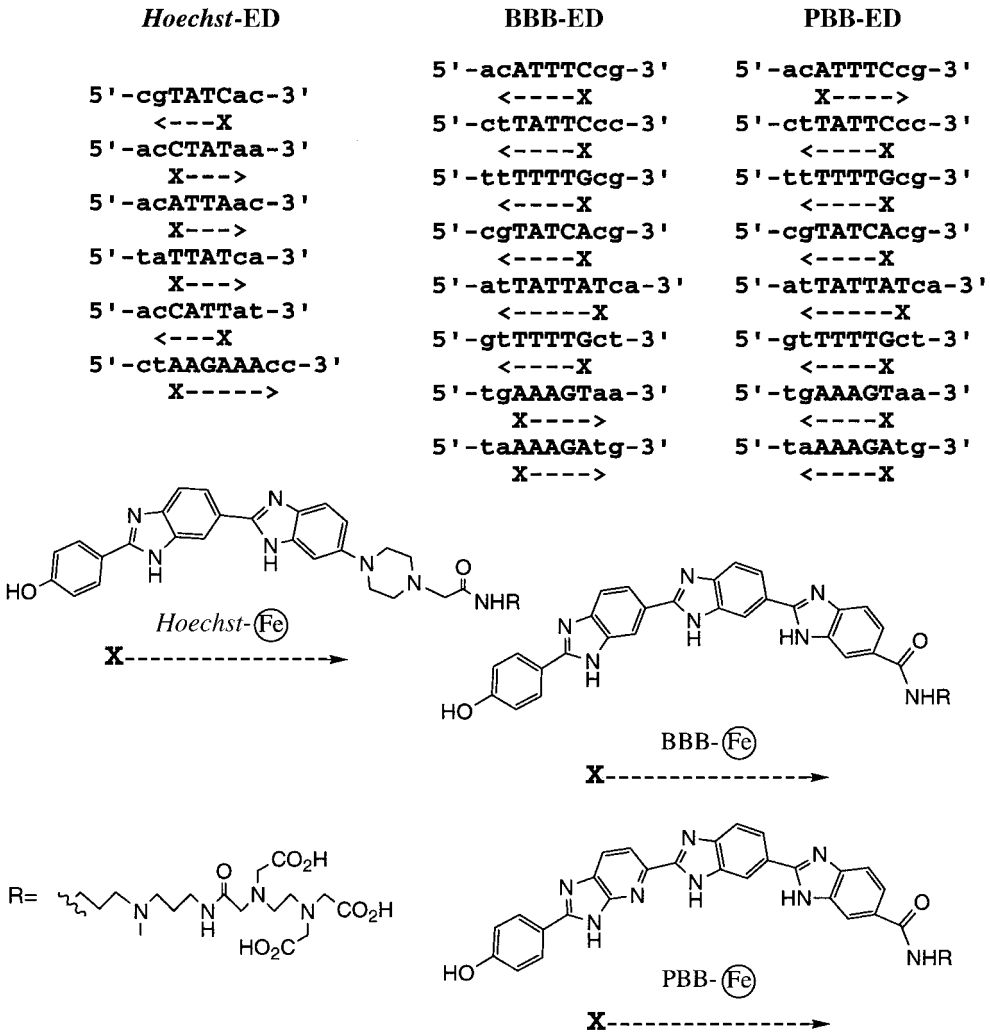

Fig. 7. *Ligand binding site and orientation summary for* Hoechst-*ED, BBB-ED, and PBB-ED*

◀

Fig. 6. a) *MPE-Fe^{II} Footprinting of BBB-Dp* (**3-Dp**) *and PBB-Dp* (**4-Dp**) *on the 5′-PCR-labeled 3991 – 4143 segment of PBr322. Lanes 1* and *18:* intact 5′-labeled DNA; *Lanes 2 – 3* and *16 – 17:* A and G reactions; *Lanes 4* and *15:* MPE-Fe^{II} digestion of DNA in the absence of ligand; *Lanes 5 – 9:* 0.5, 1, 10, 20, and 40 μM BBB-Dp; *Lanes 10 – 14:* 0.5, 1, 10, 20, and 40 μM PBB-Dp. b) *Affinity cleavage of the 5′-PCR-labeled 3991 – 4143 segment of PBr322 with BBB-ED* (**3-ED**) *and PBB-ED* (**4-ED**). *Lanes 1* and *13:* intact 5′-labeled DNA; *Lanes 2 – 3* and *11 – 12:* A and G reactions; *Lanes 4* and *11:* MPE-Fe^{II} digestion of DNA in the absence of ligand; *Lanes 5 – 7:* 0.5, 1, and 5 μM BBB-ED; *Lanes 8 – 10:* 0.5, 1, and 10 μM PBB-ED. c) *Binding sites* (in bold) *as determined by MPE-Fe^{II} footprinting, shown on the 5′- and 3′-end-labeled 3991 – 4143 segment of pBr-322*. Bar heights are proportional to the relative protection from cleavage at each bond. Shown are the protection patterns for 10 μM BBB-Dp (**3-Dp**) and 10 μM PBB-Dp (**4-Dp**). d) *Affinity-cleavage patterns for* 5 μM *BBB-ED* (**3-ED**) *and 5* μM *PBB-ED* (**4-ED**) *on the 3991 – 4143 segment of PBr322*. Line heights are proportional to the relative cleavage at each band.

NMR Spectra were recorded with TMS ($\delta = 0$ ppm) as internal standard on a *Varian Mercury 300* (^{1}H: 300 MHz, ^{13}C: 75 MHz), or on a *Varian Mercury 500* (^{13}C: 125 MHz) spectrometer; chemical shifts δ are given in ppm. High-resolution mass spectra (HR-MS) were performed by *Mass Consortium Inc.*, San Diego, CA.

2. Synthesis of *Hoechst*-ED (1-ED). – *Ethyl 2-(4-{2-[2-(4-methoxyphenyl)-1*H*-benzimidazol-6-yl]-1*H*-benzimidazol-6-yl}piperazin-1-yl)acetate* (**8**): *5-chloro-2-nitroaniline* (**6**; 2 g, 12 mmol) and piperazine (2.6 g, 30 mmol, 2.5 equiv.) were combined in DMF (23 ml), and K_2CO_3 (1.4 g) was added. The mixture was heated to 130° for 8 h. Upon cooling, the mixture was poured into H_2O and extracted 3 times with AcOEt (100 ml). The org. extracts were dried (Na_2SO_4) and evaporated to give 2-nitro-5-(piperazin-1-yl)aniline. The crude piperazine (155 mg, 690 μmol) was dissolved in DMF (1 ml) and DIEA (0.5 ml), and ethyl bromoacetate (85 μl, 760 μmol, 1.1 equiv.) was added dropwise. The mixture was stirred overnight at r.t. The mixture was poured into H_2O and extracted 3 times with AcOEt (20 ml). The org. extracts were dried (Na_2SO_4) and evaporated to give ethyl 4-(3-amino-4-nitrophenyl)piperazinecarboxylate. The crude ethyl ester (20 mg, 68 μmol) was dissolved in AcOEt (3 ml), and excess 10% Pd-C (100 mg) was added. The mixture was stirred under an atmosphere of H_2 for 1 h, and then filtered over *Celite* and concentrated *in vacuo* to give the crude *ethyl 4-(3,4-diaminophenyl)piperazinecarboxylate* (**7**; 17 mg, 63 μmol), which was immediately coupled with aldehyde **9** (16 mg, 63μmol) by the same procedure for the preparation of **12** from **9** and **11** (*vide infra*). FC (SiO_2; 10% MeOH/AcOEt) gave **8** (15 mg, 29 μmol, 4% overall). UV (H_2O): 260, 344 (42,000). ^{1}H-NMR ((D$_6$)DMSO, 300 MHz): 1.21 (*t*, *J* = 7.5, 3 H); 2.48 (*d*, *J* = 1.5, 2 H); 2.67 (*m*, 4 H); 2.95 (*q*, *J* = 6.9, 2 H); 3.27 (*m*, 2 H); 3.83 (*s*, 3 H); 4.07 (*q*, *J* = 7.5, 2 H); 6.89 (*d*, *J* = 8.4, 2 H); 7.10 (*d*, *J* = 9.0, 4 H); 7.20–7.80 (*m*, 2 H); 8.14 (*d*, *J* = 8.1, 4 H). HR-MS (MALDI-FTMS): 511.2472. ($C_{29}H_{31}N_6O_3^+$, $[M+H]^+$; calc. 511.2452).

*2-((Carboxymethyl){2-[(carboxymethyl)({*N*-[3-({3-[2-(4-{2-[2-(4-hydroxyphenyl)-1*H*-benzimidazol-6-yl]-1*H*-benzimidazol-6-yl}-piperazin-1-yl)acetylamino]propyl}methylamino)propyl]carbamoyl}methyl)amino]ethyl}-amino)acetic Acid* (**1-ED**). Compound **8** (15 mg, 29 μmol) was hydrolyzed with 48% HBr (2 ml) for 1 h at 130°. Evaporation gave a crude acid, which was carried forward without further purification. The acid was coupled with bis(3-aminopropyl)methylamine by the same procedure described for the preparation of **3-NH$_2$** to produce **1-NH$_2$** (7 mg, 41%). Excess ethylenediaminetetraacetic acid (EDTA) dianhydride (50 mg, 195 μmol) was dissolved in DMSO/NMP (1 ml) and DIEA (1 ml) by heating at 55° for 5 min. The dianhydride soln. was added to **1-NH$_2$** (7 mg, 12 μmol) dissolved in DMSO (50 μl). The mixture was heated (55°, 25 min), and the remaining EDTA anhydride was hydrolyzed (0.1M NaOH, 3 ml, 55°, 10 min). Aq. CF_3COOH (TFA) (0.1 wt-%/*v*) was added to adjust the total volume to 8 ml, and the soln. was purified directly by RP-HPLC (20% MeCN/0.1% aq. TFA) to provide **1-ED** (0.5 mg, 5%). UV (H_2O): 261, 346 (42,000). ^{1}H-NMR ((D$_6$)DMSO, 300 MHz): 1.83 (*m*, 4 H); 2.49 (*m*, 15 H); 2.75 (*m*, 4 H); 2.91 (*m*, 4 H); 3.15 (*m*, 10 H); 6.95 (*d*, *J* = 8.4, 2 H); 7.14 (*m*, 2 H); 7.60 (*m*, 2 H); 7.75 (*m*, 2 H); 8.06 (*d*, *J* = 7.5, 2 H); 8.35 (br. *s*, 4 H); 10.15 (br. *s*, 3 H). HR-MS (MALDI-FTMS): 892.4052 ($C_{43}H_{55}N_{11}O_9Na^+$, $[M+Na]^+$; calc. 892.4076).

3. Synthesis of the BBB (3) and PBB (4) Trimers. – *2-{2-[2-(4-Methoxyphenyl)-1*H*-benzimidazol-6-yl]-1*H*-benzimidazol-6-yl}-1*H*-benzimidazole-6-carbonitrile* (**12**). A soln. of *2-(4-methoxyphenyl)-1*H*-benzimidazole-6-carbaldehyde* (**9**; 44 mg, 170 μmol) and **11** (44 mg, 170 μmol) in $PhNO_2$ (1 ml) was stirred at 150° under Ar for 19 h. Evaporation of the solvent and trituration with CH_2Cl_2 and Et_2O gave a brown solid after filtration. Purification by RP (*C18*) silica-gel chromatography (35% MeCN/0.1% aq. TFA) gave **12** (51 mg, 62%). UV (MeOH): 250, 341 (30,000). ^{1}H-NMR ((D$_6$)DMSO, 300 MHz): 3.82 (*s*, 3 H); 7.13 (*m*, 3 H); 7.67 (*m*, 1 H); 7.80 (*m*, 2 H); 8.18 (*m*, 6 H); 8.49 (*m*, 1 H). HR-ES-MS: 482.1799. ($C_{29}H_{20}N_7O^+$, $[M+H]^+$; calc. 482.1729).

N-*[3-(Dimethylamino)propyl]-2-{2-[2-(4-methoxyphenyl)-1*H*-benzimidazol-6-yl]-1*H*-benzimidazol-6-yl}-1*H*-benzimidazole-6-carboxamide* (**3-Dp**). A soln. of **12** (20 mg, 40 μmol) in 48% HBr (1.5 ml) was heated to 150° for 4 h. The soln. was cooled to r.t. and evaporated to dryness. To a soln. of crude acid (20 mg, 39 μmol) in DMF (1 ml) was added HOBt (10 mg, 84 μmol, 2.1 equiv.) and DCC (17 mg, 84 μmol, 2.1 equiv.), and the mixture was allowed to stir for 30 min. The white precipitate was filtered off and DIEA (0.5 ml) and 3-(dimethylamino)propylamine (0.25 ml) were added dropwise. The mixture was stirred at r.t. for 5 h and then concentrated *in vacuo*. Purification by RP-HPLC (30% MeCN/0.1% aq. CF_3COOH) gave **3-Dp** (8 mg, 36% overall). UV (H_2O): 250, 346(30,000). ^{1}H-NMR ((D$_6$)DMSO, 300 MHz): 1.56–1.81 (*m*, 2 H); 2.76 (*s*, 3 H); 2.78 (*s*, 3 H); 3.00–3.25 (*m*, 4 H); 3.82 (*s*, 3 H); 7.13 (*m*, 3 H); 7.67 (*m*, 1 H); 7.80 (*m*, 2 H); 8.16 (*m*, 5 H); 8.46 (*m*, 2 H). HR-MS (MALDI-TOF): 585.2731 ($C_{34}H_{33}N_8O_2^+$, $[M+H]^+$; calc. 585.2721).

N-*{3-[(3-Aminopropyl)methylamino]propyl}-2-{2-[2-(4-methoxyphenyl)-1*H*-benzimidazol-6-yl]-1*H*-benzimidazol-6-yl}-1*H*-benzimidazole-6-carboxamide* (**3-NH$_2$**). To a soln. of crude acid derived from hydrolysis of **12** in the previous step (20 mg, 39 μmol) in DMF (1 ml) was added HOBt (10 mg, 84 μmol, 2.1 equiv.) and DCC (17 mg, 84 μmol, 2.1 equiv.), and the mixture was allowed to stir for 30 min. The white precipitate was filtered off and DIEA (0.5 ml) and (3-aminopropyl)methylamine (0.25 ml) were added dropwise. The mixture was

stirred at r.t. for 5 h and then concentrated *in vacuo*. Purification by RP-HPLC (30% MeCN/0.1% aq. CF_3COOH) gave **3-NH$_2$** (11 mg, 33% overall). UV (H_2O) 255, 348 (30,000). ^{1}H-NMR ((D$_6$)DMSO; 300 MHz): 1.50–1.87 (*m*, 4 H); 2.52–2.81 (*m*, 7 H); 3.84 (*s*, 3 H); 5.54 (*m*, 2 H); 7.15 (*d*, *J* = 8.1, 2 H); 7.84 (*m*, 5 H); 8.16 (*m*, 4 H); 8.45 (*s*, 2 H). HR-MS (MALDI-TOF): 628.3162 ($C_{36}H_{38}N_9O_2^+$, $[M+H]^+$; calc. 628.3148).

*2-((Carboxymethyl){2-[(carboxymethyl)({*N*-[3-({3-[(2-{2-[2-(4-methoxyphenyl)-1*H*-benzimidazol-6-yl]-1*H*-benzimid-azol-6-yl}-1*H*-benzimidazol-6-yl)carbonylamino]propyl}methylamino)propyl]carbamoyl}methyl)-amino]ethyl}amino)acetic Acid* (**3-ED**). Excess EDTA dianhydride (50 mg, 195 μmol) was dissolved in DMSO/*N*-methylphthalimide (NMP) (1 ml) and DIEA (1 ml) by heating at 55° for 5 min. The dianhydride soln. was added to **3-NH$_2$** (2 mg, 2 μmol) dissolved in DMSO (50 μl). The mixture was heated (55°, 25 min) and the remaining EDTA-anhydride hydrolyzed (0.1M NaOH, 3 ml, 55°, 10 min). Aq. CF_3COOH (0.1 wt-%/*v*) was added to adjust the total volume to 8 ml, and the soln. was purified directly by RP-HPLC (20% MeCN/0.1% aq. CF_3COOH) to provide **3-ED** (1.0 mg, 38%). UV (H_2O): 253, 346 (30,000). ^{1}H-NMR ((D$_6$)DMSO, 300 MHz): 1.80 (*m*, 2 H); 1.93 (*m*, 2 H); 2.49 (*d*, *J* = 1.5, 3 H); 2.77 (*m*, 8 H); 3.11 (*m*, 12 H); 3.98 (*s*, 3 H); 7.13 (*d*, *J* = 8.0, 2 H); 7.78 (*m*, 5 H); 8.20 (*m*, 4 H); 8.45 (*s*, 2 H). HR-MS (MALDI-TOF): 924.3738 ($C_{46}H_{51}N_{11}O_9Na^+$, $[M+Na]^+$; calc. 924.3763).

*2-{2-[2-(4-Methoxyphenyl)-1*H*-imidazo[4,5-*b*]pyridin-5-yl]-1*H*-benzimidazol-6-yl}-1*H*-benzimidazole-6-carbonitrile* (**13**). A soln. of aldehyde **10** (40 mg, 160 μmol) and **11** (41 mg, 16 μmol) in $PhNO_2$ (1 ml) was stirred at 150° under Ar for 19 h. Evaporation of the solvent and trituration with CH_2Cl_2 and Et_2O gave a brown solid after filtration. Purification by RP (*C18*) silica-gel chromatography (35% MeCN/0.1% aq. CF_3COOH) gave **13** (40 mg, 51%). UV (MeOH): 251, 360 (45,000). ^{1}H-NMR ((D$_6$)DMSO, 300 MHz): 3.83 (*s*, 3 H); 7.15 (*d*, *J* = 10.0, 2 H); 7.65 (*d*, *J* = 8.2, 1 H); 7.80 (*d*, *J* = 8.1, 1 H); 7.88 (*d*, *J* = 8.1, 1 H); 7.80 (*d*, *J* = 8.0, 1 H); 8.20–8.40 (*m*, 6 H); 8.55 (*m*, 1 H). HR-MS (MALDI-TOF): 483.1656 ($C_{28}H_{19}N_8O^+$, $[M+H]^+$; calc. 483.1682).

N-*{3-(Dimethylamino)propyl}-2-{2-[2-(4-hydroxyphenyl)-1*H*-imidazo[4,5-*b*]pyridin-5-yl]-1*H*-benzimida-zol-6-yl}-1*H*-benzimidazole-6-carboxamide* (**4-Dp**). A soln. of **13** (20 mg, 40 μmol) in 48% HBr was heated to 150° for 1 h. The soln. was cooled to r.t. and evaporated to dryness. To a soln. of crude acid (20 mg, 39 μmol) in DMF (1 ml) was added HOBt (10 mg, 84 μmol, 2.1 equiv.) and DCC (17 mg, 84 μmol, 2.1 equiv.) and the mixture was allowed to stir for 30 min. The white precipitate was filtered off, and DIEA (0.50 ml) and 3-(dimethylamino)propyl amine (0.25 ml) were added dropwise. The mixture was stirred at r.t. for 5 h and then concentrated *in vacuo*. Purification by RP-HPLC (30% MeCN/aq. CF_3COOH (0.1 wt-%/*v*)) gave **4-Dp** (5 mg, 25% overall). UV (H_2O): 251, 362 (45,000). ^{1}H-NMR ((D$_6$)DMSO, 300 MHz): 1.56–1.81 (*m*, 2 H); 2.76 (*s*, 3 H); 2.78 (*s*, 3 H); 3.00–3.25 (*m*, 4 H); 6.98 (*d*, *J* = 8.0, 5 H); 8.14 (*m*, 7 H). HR-MS (MALDI-TOF): 572.2505. ($C_{32}H_{31}N_9O_2^+$, $[M+H]^+$; calc. 572.2522).

N-*{3-[(3-Aminopropyl)methylamino]propyl}-2-{2-[2-(4-hydroxyphenyl)-1*H*-imidazo[4,5-*b*]pyridin-5-yl]-1*H*-benzimidazol-6-yl}-1*H*-benzimidazole-6-carboxamide* (**4-NH$_2$**). To a soln. of crude acid derived from hydrolysis of **13** in the previous step (20 mg, 39 μmol) in DMF (1 ml) was added HOBt (10 mg, 84 μmol, 2.1 equiv.) and DCC (17 mg, 84 μmol, 2.1 equiv.), and the mixture was allowed to stir for 30 min. The white precipitate was filtered off, and DIEA (0.50 ml) and (3-aminopropyl)methylamine (0.25 ml) were added dropwise. The mixture was stirred at r.t. for 5 h and then concentrated *in vacuo*. Purification by RP-HPLC (30% MeCN/0.1% aq. CF_3COOH) gave **4-NH$_2$** (10 mg, 30% overall). UV (H_2O): 250, 362 (45,000). ^{1}H-NMR (CD_3CN, 300 MHz): 1.50–2.05 (*m*, 4 H); 2.81 (*s*, 3 H); 3.15–3.50 (*m*, 8 H); 6.14 (*d*, *J* = 8.5, 5 H); 7.14 (*m*, 7 H). HR-MS (MALDI-TOF): 615.2962. ($C_{34}H_{35}N_{10}O_2^+$, $[M+H]^+$; calc. 615.2944).

*2-((Carboxymethyl){2-[(carboxymethyl)({*N*-[3-({3-[(2-{2-[2-(4-hydroxyphenyl)-1*H*-imidazo[4,5-*b*]pyri-din-5-yl]benzimidazol-6-yl}-1*H*-benzimidazol-6-yl)carbonylamino]propyl}methylamino)propyl]carbamoyl}-methyl)amino]ethyl}amino)acetic* Acid (**4-ED**). Excess EDTA dianhydride (50 mg, 195 μmol) was dissolved in DMSO/NMP (1 ml) and DIEA (1 ml) by heating at 55° for 5 min. The dianhydride soln. was added to **4-NH$_2$** (2 mg, 2 μmol) dissolved in DMSO (50 μl). The mixture was heated (55°, 25 min), and the remaining EDTA anhydride was hydrolyzed (0.1M NaOH, 3 ml, 55°, 10 min). Aq. CF_3COOH (0.1 wt-%/*v*) was added to adjust the total volume to 8 ml, and the soln. was purified directly by RP-HPLC (20% MeCN/0.1% aq. CF_3COOH) to provide **4-ED** (0.5 mg, 28%). UV (H_2O): 250, 358 (45,000). ^{1}H-NMR ((D$_6$)DMSO, 300 MHz): 1.82 (*m*, 2 H); 1.91 (*m*, 2 H); 2.47 (*d*, *J* = 1.5, 3 H); 2.80–2.88 (*m*, 8 H); 3.40 (*m*, 12 H); 3.80 (*s*, 3 H); 6.23 (*d*, *J* = 8.0, 5 H); 7.15 (*m*, 7 H). HR-MS (MALDI-TOF): 889.3707. ($C_{44}H_{49}N_{12}O_9^+$, $[M+H]^+$; calc. 889.3740).

4. Synthesis of the HBB Trimer 5. – *2-[2-(4-Chloro-7-methoxy-2-methyl-1*H*-benzimidazol-6-yl)-1*H*-benzimidazol-6-yl]-1*H*-benzimidazole-6-carbonitrile* (**16**). A soln. of **15** (117 mg, 520 μmol) and **11** (130 mg, 520 μmol) in $PhNO_2$ (5.2 ml) was stirred at 150° for 18 h. After evaporation, the residue was triturated with AcOEt, dissolved in MeOH, and filtered. The filtrate was evaporated to yield **16** (184 mg, 78%). UV (MeOH):

245, 336 (37445). ^{13}C-NMR (CD_3OD, 125 MHz): 156.29; 151.71; 126.22; 124.29; 123.05; 122.96; 122.03; 120.82; 105.06; 61.79; 14.43. HR-ESI-MS: 454.1167 ($C_{24}H_{17}ClN_7O^+$, $[M+H]^+$; calc. 454.1183).

N-*[3-(Dimethylamino)propyl]-2-[2-(4-chloro-7-hydroxy-2-methyl-1*H*-benzimidazol-6-yl)-1*H*-benzimidazol-6-yl]-1*H*-benzimidazole-6-carboxamide* (**5**). A soln. of **16** (33 mg, 73 μmol) in 48% HBr (1.5 ml) was refluxed for 30 min. Evaporation and azeotropic destillation with benzene (3×) afforded the crude hydroxy acid. To a soln. of this acid in DMF (2 ml) and DIEA (0.5 ml) were added DCC (31.8 mg, 153 μmol, 2.1 equiv.) and HOBt (18.7 mg, 153 μmol, 2.1 equiv.), and the mixture was stirred at r.t. for 20 min. 3-(dimethylamino)-propylamine (0.25 ml) was added, and the mixture was stirred at r.t. for 3 h. After addition of 0.1% CF_3COOH/H_2O (2 ml), the solution was filtered and purified by HPLC (25% MeCN/0.1% TFA) to give **5** (3.9 mg, 20%). HR-ESI-MS: 543.2042 ($C_{28}H_{28}ClN_8O_2^+$, $[M+H]^+$; calc. 543.2024).

5. Preparation and Labeling of DNA Restriction Fragment. – The plasmid pBR322 was linearized with EcoRI and RsaI and then treated with Sequenase v. 2.0, deoxyadenosine 5′-[α-^{32}P]triphosphate, and thymidine 5′-[α-^{32}P]triphosphate. The 3′-end labeled fragment was loaded onto a 7% nondenaturing polyacrylamide gel. The desired 519 base-pair band was visualized by autoradiography and isolated. Chemical sequencing reaction performed according to published methods.

Sequences of the PCR primers for plasmid pBR322: Primer P1: 5′-GTACTCAACCAAGTCATTCTG-3′, Primer P2: 5′-GGAAGAGTATGAGTATTCAAC-3′. Primer 2 was 5′-radiolabeled with γ-^{32}P-[ATP] using T4-polynucleotide kinase. PCR amplification in the presence of P1, P2 (labeled), plasmid pBR322, and Taq polymerase gave a 298 bp DNA fragment that was purified on a 6% nondenaturating polyacrylamide gel.

Sequences of the PCR primers for plasmid pJT3: Primer P1: 5′-GCAACTGTTGGGAAGGGCGAT-3′, Primer P2: 5′-TTAAGACGCTACGACGCTAGCT-3′. Primer 2 was 5′-radiolabeled with γ-^{32}P-[ATP] using T4-polynucleotide kinase. PCR amplification in the presence of P1, P2 (labeled), plasmid pJT3, and Taq polymerase gave a 286 bp DNA fragment that was purified on a 6% nondenaturating polyacrylamide gel.

6. MPE·Fe^{II} Footprint Titrations. – All MPE footprinting reactions were performed in a total volume of 40 μl containing 5′- or 3′-^{32}P-radiolabeled DNA fragments (17,000 cpm) and final concentrations of 25 mM *Tris* acetate, 10 mM NaCl, 100 μM/bp calf thymus DNA, pH 7.0, and either 0.1 to 100 μM polyamide or polybenzimidazole ligand. The solns. were allowed to equilibrate for 1–3 h at 22°. After addition of 4 μl of 50 μM MPE-Fe^{II} (freshly prepared from 100 μl of a 100 μM MPE soln. and 100 μl of 100 μM $Fe(NH_4)_2(SO_4)_2\cdot 6H_2O$ soln., the mixtures were incubated for 5 min. Cleavage was initiated by addition of 4 μl of a 50 mM DTT soln. and allowed to proceed for 14 min at r.t. Reactions were stopped by EtOH precipitation. The precipitates were resuspended in 1× TBE/80% formamide loading buffer, denaturated by heating at 85° for 10 min, and cooled on ice. The reaction products were separated by electrophoresis on a 6% polyacrylamide gel in 1× TBE at 2000 V for 1 h. Gels were dried on a slab dryer and exposed to a photostimulatable storage phosphor imaging plate (*Kodak Storage Phosphor Screen SO230* obtained from *Molecular Dynamics*) in the dark at 22° for 12 to 24 h. The data from the storage screens were obtained using a *Molecular Dynamics 400S PhosphorImager* and analyzed by volume integration of the target sites and reference blocks using the *ImageQuant* version 3.3. software.

7. Affinity-Cleavage Titrations. – All affinity-cleavage-titration reactions were performed in a total volume of 40 μl containing 5′- or 3′-^{32}P-radiolabeled DNA fragments (17,000 cpm) and final concentrations of 25 mM *Tris* acetate, 20 mM NaCl, 100 μM/bp calf thymus DNA, pH 7.0, and either 0.1 to 10 μM polyamide or polybenzimidazole ligand. The solns. were allowed to equilibrate for 1–3 h at 22°. After addition of 4μl of 100 μM $Fe(NH_4)_2(SO_4)\cdot 6H_2O$ soln., the mixtures were incubated for 5 min. Cleavage was initiated by addition of 4μl of a 50 mM DTT soln. and allowed to proceed for 30 min at r.t. Reactions were stopped by EtOH precipitation. The precipitates were resuspended in 1× TBE/80% formamide loading buffer, denaturated by heating at 85° for 10 min, and cooled on ice. The reaction products were separated by electrophoresis on a 6% polyacrylamide gel in 1× TBE at 2000 V for 1 h. Gels were dried on a slab dryer and exposed to a photostimulatable storage phosphor imaging plate (*Kodak Storage Phosphor Screen SO230* obtained from *Molecular Dynamics*) in the dark at 22° for 12 to 24 h. The data from the storage screens were obtained using a *Molecular Dynamics 400S PhosphorImager* and analyzed by volume integration of the target sites and reference blocks using the *ImageQuant* version 3.3. software.

REFERENCES

[1] P. B. Dervan, *Science* **1986**, *232*, 464.
[2] D. E. Wemmer, P. B. Dervan, *Curr. Opin. Struct. Biol.* **1997**, *7*, 355.

[3] C. Zimmer, U. Wahnert, *Prog. Biophys. Mol. Biol.* **1986**, *47*, 31.
[4] M. L. Kopka, C. Yoon, D. Goodsell, P. Pjura, R. E. Dickerson, *Proc. Natl. Acad. Sci. U.S.A.* **1985a**, *82*, 1376.
[5] M. L. Kopka, C. Yoon, D. Goodsell, P. Pjura, R. E. Dickerson, *J. Mol. Biol.* **1985b**, *183*, 553.
[6] M. Coll, C. A. Fredrick, A. H. Wang, A. Rich, *Proc. Natl. Acad. Sci. U.S.A.* **1987**, *84*, 8385.
[7] R. E. Klevit, D. E. Wemmer, R. R. Reid, *Biochemistry*, **1986**, *25*, 3296.
[8] J. G. Pelton, D. E. Wemmer, *Biochemistry* **1988**, *27*, 8088.
[9] J. G. Pelton, D. E. Wemmer, *Proc. Natl. Acad. Sci. U.S.A*. **1989**, *86*, 5723.
[10] J. G. Pelton, D. E. Wemmer, *J. Am. Chem. Soc* **1990**, *112*, 1393.
[11] R. F. Martin, N. Holmes, *Nature*, **1983**, *302*, 452.
[12] K. D. Harshman, P. B. Dervan, *Nucl. Acids Res.* **1985**, *13*, 4825.
[13] M. Teng, N. Usman, C. A. Frederick, A. Wang, *Nucl. Acids Res.* **1988**, *16*, 2671.
[14] P. E. Pjura, G. Kazimierz, R. E. Dickerson, *J. Mol. Biol.* **1987**, *197*, 257.
[15] S. Kumar, B. Yadagiri, J. Zimmermann, R. T. Pon, J. W. Lown, *J. Biomol. Struct. Dyn.* **1990**, *8*, 331.
[16] W. S. Wade, M. Mrksich, P. B. Dervan, *J. Am. Chem. Soc* **1992**, *114*, 8783.
[17] M. Mrksich, W. S. Wade, T. J. Dwyer, B. H. Geierstanger, D. E. Wemmer, P. B. Dervan, *Proc. Natl. Acad. Sci. U.S.A.* **1992**, *89*, 7568.
[18] P. B. Dervan, R. W. Burli, *Curr. Opin. Chem. Biol.* **1999**, *3*, 688.
[19] S. Frau, J. Bernadou, B. Meunier, *Bull. Soc. Chim. Fr.* **1996**, *133*, 1053.
[20] M. Kubista, B. Akerman, B. Norden, *Biochemistry* **1987**, *26*, 4545.
[21] L. Wang, C. Bailly, A. Kumar, D. Ding, M. Bajic, D. W. Boykin, W. D. Wilson, *Proc. Natl. Acad. Sci. U.S.A*. **2000**, *97*, 12.
[22] J. W. Lown, in 'Advances in DNA Sequence Specific Agents', **1998**, *3*, 67.
[23] M. W. Van Dyke, P. B. Dervan, *Nucl. Acids Res.* **1983**, *11*, 5555.
[24] M. Lee, P. H. Spotts, J. Eckert, C. Walker, J. A. Nobles, *Heterocycles*, **1991**, *32*, 2093.
[25] M. P. Singh, T. Joseph, S. Kumar, Y. Bathini, L. J. Lown, *Chem. Res. Toxicol.*, **1992**, *5*, 597.
[26] A. Czarny, W. D. Wilson, J. Boykin, *J. Heterocycl. Chem.* **1996**, *33*, 1393.
[27] D. H. Herman, E. E Baird, P. B. Dervan, *J. Am. Chem. Soc* **1998**, *120*, 1382.
[28] A. Tanaka, K. Ito, S. Nishino, Y. Motoyama, H. Takasugi, *Chem. Pharm. Bull.* **1994**, *42*, 560.
[29] J. W. Trauger, E. E. Baird, M. Mrksich, P. B. Dervan, *J. Am. Chem. Soc.* **1996**, *118*, 6160.
[30] Gas-phase *ab initio* HF/6-31G** energy minimization; *Jaguar* software package, *Schrödinger, Inc*.

Received May 22, 2000